

# Threshold ionization of atoms by electron and positron impact

Jan-Michael Rost

Fakultät für Physik, Universität Freiburg, Hermann–Herder–Str. 3, D–79104 Freiburg, Germany

Received 12 January 1995, in final form 11 May 1995

**Abstract.** In two recent letters results for threshold ionization of hydrogen by electron impact (Rost J M 1994 *Phys. Rev. Lett.* 72 1998) and positron impact (Rost J M and Heller E J 1994 *Phys. Rev. A* 49 R4289) were communicated. The results were obtained by calculating the *S*-matrix semiclassically in Feynman's path integral formalism. This paper gives a more complete account of the theoretical method. Moreover, it is shown how the ionization cross section of atomic targets other than hydrogen can be expressed with the hydrogen cross section through a scaling relation. This demonstrates the universality of the threshold behaviour.

## 1. Introduction

The motivation for this work, more specifically, for using a semiclassical approach to understand threshold ionization, is threefold. Low-energy inelastic scattering has been described within different frameworks, dependent on the process under consideration. For excitation and charge transfer (for instance in ion–atom collisions) coupled channel calculations with basis sets centred on the target and the projectile have been successful (see, for example, Burke and Berrington 1993). Ionization in the low- and intermediate-energy regime is much more difficult to describe since a formulation of observables with discretized continuum states does not necessarily converge for long-range potentials. Only recently the 'convergent close-coupling method' (CCC) has provided numerically converged cross sections and the asymmetry parameter for ionization of hydrogen at about 10 eV excess energy and higher (Bray and Stelbovics 1993). For small excess energies it has not been possible to obtain converged results since the accuracy depends sensitively on the number of excitation channels included. In the limit  $E \rightarrow 0$  an infinite number of these states would be necessary for an accurate ionization cross section. Hence, even the spectacular success of the CCC method over a wide energy range still leaves the threshold region as a theoretically unsolved problem. This is one motivation for the semiclassical *S*-matrix theory as presented here.

Another motivation is the notorious difficulty with final states containing more than two charged fragments in the continuum. Quantum mechanically there is a big difference between these states and states representing 'free' particles in problems with short-range forces (Rosenberg 1974, Brauner *et al* 1989, Berakdar and Briggs 1994). In contrast, semiclassically there is no conceptual difference in describing charged or neutral particles in the continuum. Moreover, it is not necessary to know the form of the continuum final states, for instance, in an ionization calculation. To demonstrate these conceptual advantages of semiclassical scattering theory, in particular for long-range potentials, is a second motivation for this work.

Finally, a third motive arises from the historical perspective on threshold ionization. Since Wannier's fascinating paper on the mechanism of threshold ionization based on purely classical reasoning in 1953 there has been a continuing discussion as to whether Wannier's ionization scenario is correct and whether a classical approach is justified. Important contributions can be found in the papers by Peterkop (1971), Rau (1971), Temkin (1982), Feagin (1984) and Crothers (1986). The semiclassical  $S$ -matrix description naturally contains the classical result as a limit and can shed new light on the accuracy and justification of the classical limit.

An overview of the literature about threshold ionization has been given in the review articles by Read (1984a), Rau (1984), Grujic (1986) and Lubell (1994). Recent developments include the time-dependent evolution of wavepackets on the Wannier ridge (Kazansky and Ostrovsky 1993) and the classical and quantum mechanical investigation of the so-called 's-wave model' for helium (Handke *et al* 1993). Not specifically designed for the threshold but very successful in the description of differential cross sections at small excess energies is the approach developed initially by Brauner *et al* (1989) with important improvements by Berakdar and Briggs (1994) and the application to photoionization by Maulbetsch and Briggs (1992). Rather than repeating the overview of the literature in detail, here we prefer to put the semiclassical  $S$ -matrix approach into a broader perspective.

Semiclassical approximations have existed almost as long as the quantum theory itself. They have served two rather different purposes: first, to explore the classical limit of quantum mechanics and to gain more insight into the nature of quantum phenomena. Second, to develop a theory that provides reliable approximations for cases in which it is not possible to solve the full problem quantum mechanically. Certainly, the formulation of the semiclassical propagator initiated by van Vleck (1928) and completed by Maslov (see Maslov and Fedoriuk 1981) and Gutzwiller (e.g. Gutzwiller 1990) belongs to the first category. Within the second category the WKB approach has been most successful in different areas of physics. The essentially one-dimensional theory has led to useful results in times where we lacked the computer power to treat complicated, more dimensional problems. For scattering problems a logical application has been the calculation of WKB phase shifts for elastic scattering, pioneered by Ford and Wheeler (1959). Subsequent topics of semiclassical scattering theory have dealt with problems that fulfil the traditional criterion for the application of semiclassical methods, that is, that the relative change of the wavelength in the physical problem is small. An example is nucleus-nucleus scattering where the heavy masses and the large charges of the nuclei provide a short de Broglie wavelength (Brink 1982).

With the improvement of computers, even the most general semiclassical formulation by van Vleck has become computationally feasible and thus conceptually interesting again (Sepulveda and Heller 1994). Miller showed in the seventies that semiclassical approximations for the Green's function itself can lead to remarkable results for reactive scattering in molecular complexes, whose dynamics cannot be characterized by short wavelengths (Miller 1974, 1975 and references therein). For the energy spectrum of bound systems Gutzwiller formulated the 'trace formula' (Gutzwiller 1990). Together with the 'cycle expansion', a resummation method, the trace formula was used recently by Wintgen *et al* (1992) to show that helium can be quantized semiclassically despite the initial failure of the old quantum theory some 60 years ago. Using the van Vleck propagator directly in the time domain Tomsovic and Heller (1994) obtained spectra and selected eigenstates of classically chaotic systems semiclassically to a good accuracy. Other recent applications of semiclassical theory include electron transport problems in mesoscopic devices, quantum dots etc (see for instance Baranger *et al* 1993). These are only a few, although spectacular,

examples from a substantial body of work that has advanced semiclassical theories so much in the last few years that it might be justified to speak of a revival of the semiclassical perspective. The revival is fueled by new experiments with excellent energy resolution even for highly excited spectra (Main *et al* 1986). Their interpretation needs a theoretical description and understanding of dynamics in the limit of large quantum numbers. This implies a natural demand for further developing semiclassical methods. An impressive example of such a development is the understanding of a complicated spectrum of hydrogen in a magnetic field. Accompanied by exact quantum mechanical treatments (see the reviews by Wintgen and Friedrich (1989) and Hasegawa *et al* (1989) as well as the special issue of *J. Phys. B: At. Mol. Opt. Phys.* **27** (1994)) the semiclassical approach was pioneered by Wintgen (1987, 1988) and Delos (Du and Delos 1987).

Here we will present a semiclassical formulation for inelastic electron-atom scattering. It is derived from the path integral representation of the  $S$ -matrix and in the form given here is especially designed to describe the threshold region of ionization. The result will be similar to Miller's 'classical  $S$ -matrix', formulated 25 years ago and applied to 2D model calculation in reactive scattering of molecules (Miller 1970, 1970b, 1970c, Rankin and Miller 1971). The major difference is the application to scattering involving the long-range Coulomb force. However, this actually improves the accuracy of the semiclassical approximation in comparison to Miller's results for molecular problems.

The paper is organized as follows. In section 2 we parametrize the ionization cross section with variables suitable for describing threshold ionization. The formulation utilizes partial waves of fixed total angular momentum  $L$ . Furthermore, based on the classical scaling properties for the Coulomb potential, we give an argument why Feynman's path integral can be evaluated semiclassically for fragmentation close to threshold  $E = 0$ . An additional substantial simplification emerges that allows the total cross section to be described ultimately with only two degrees of freedom, the radial distances  $r_i$  between the electrons and the nucleus. In section 3 the semiclassical  $S$ -matrix for ionization is explicitly derived from Miller's classical  $S$ -matrix (1974) for reactive scattering. Section 4 is devoted to an application of the semiclassical  $S$ -matrix approach to positron-hydrogen scattering. The essential features of Coulomb fragmentation will become clear in this example. In addition, we present a simple alternative derivation of the  $S$ -matrix. In section 5 we attack the problem of threshold ionization of hydrogen, the 'classical' Wannier problem. Here we will discuss in detail the differential cross section for the energy sharing between the electrons as well as the total ionization cross section and will derive the classical origin for the different behaviour of the singlet and the triplet partial wave. In section 6 we use some properties of the threshold ionization to extend the results obtained for hydrogen as a target by a simple scaling argument to valence-shell as well as to inner-shell ionization of complex atoms. Finally, in section 7, we will summarize the results and conclude with some remarks about the connection of threshold ionization ( $E > 0$ ) and resonant scattering ( $E < 0$ ).

## 2. Formal considerations for the threshold analysis

### 2.1. Irreducible decomposition of the cross section according to the constants of motion

The ionization cross section can be parametrized in many different ways (Klar and Fehr 1992). Our intention is to formulate a cross section whose variables are as close as possible to the quantities relevant for the approximations traditionally introduced when the behaviour of the scattering system is discussed close to the fragmentation threshold  $E = 0$ . To this

end we use the constants of motion of the two-electron Hamiltonian for an irreducible decomposition of the cross section. The Hamiltonian for three different particles interacting via two-body central forces preserves the total spatial angular momentum  $L$ , and parity  $\pi$ . If two of the three particles are identical (e.g. two electrons) there is an additional exchange symmetry ( $e_1 \leftrightarrow e_2$ ) which can be denoted by the net spin  $S$  that is preserved in the non-relativistic case for the identical pair ( $S = 0$  for singlet and  $S = 1$  for triplet). On the other hand, the final state in the continuum is characterized by the two electron momenta ( $\vec{p}_1, \vec{p}_2$ ). For a general three-body system we choose  $\vec{p}_1$  and  $\vec{p}_2$  to connect the two particles of the same polarity with the third particle, respectively. Another set of variables more convenient for the parametrization with the constants of motion would contain  $p_1, p_2$  and  $\theta_{12} \equiv \arccos \vec{p}_1 \vec{p}_2 / (p_1 p_2)$  through which the position of the three particles relative to each other is fixed. The position of this triangle in space is then described by a rotation with a set of Euler angles  $(\varphi, \theta, \xi) \equiv \Omega_3$ . Instead of momenta we may use energies and the energy conservation explicitly,  $\epsilon = p_1^2/2$  and  $p_2^2/2 = E - \epsilon$ , so that finally  $(\vec{p}_1, \vec{p}_2)$  is replaced by the set  $(\Omega_3, E, \epsilon, \theta_{12})$ . By integrating the triple differential cross section  $d^3\sigma / (d\Omega_3 d\cos\theta_{12} d\epsilon)$  over  $\Omega_3$  we obtain the double differential cross section (DDCs) which is differential in the angle  $\theta_{12}$  and the energy  $\epsilon$  of one electron. It can be written as a sum of partial cross sections parametrized by the total angular momentum

$$\frac{d^2\sigma^{S,\pi}(E)}{d\cos\theta_{12} d\epsilon} = \sum_L \sigma_L^{S,\pi}(E, \epsilon, \theta_{12}, \alpha') \quad (1)$$

where  $\alpha'$  denotes the initial state that we take in this paper to be the ground state (1s) of the target electron and a projectile with the energy  $\epsilon' = E - E_{1s}$ . As mentioned above, we want to start our threshold consideration from a formulation of the *cross section* in terms of the variables  $\epsilon$  and  $\theta_{12}$  traditionally used in threshold theories. By starting from the cross section (1) the approximations to be introduced for the threshold ionization will become transparent. These approximations can be motivated by evaluating the partial cross sections  $\sigma_L$  in (1) with a semiclassical  $S$ -matrix approach. Since only elements of the classical dynamics of the three-body system enter the semiclassical  $S$ -matrix, the approximations are based on the properties of the classical Hamiltonian in the limit of vanishing excess energy  $E \rightarrow 0$  and the relation to previous threshold approaches by Wannier and others will become clear.

## 2.2. Properties of the classical equations of motion of a three-body Coulomb system

A classical system of  $N$  particles interacting via two-body Coulomb forces has some remarkable properties that turn out to be important for the semiclassical description of the scattering process. They do not depend on the choice of the coordinate system but are particularly simple to derive in hyperspherical coordinates (Rost 1994b). The hyperradius  $\mathcal{R}^2 = \sum_i \mu_i r_i^2$ , composed of all mass weighted lengths of the Jacobi coordinates, measures the overall extension of the system. The mass weighting factors  $\mu_i$  are the reduced masses along the Jacobi vectors  $\vec{r}_i$ . The rest of the new coordinates spans a space of  $3N - 4$  angles  $\Omega$  on the hypersphere with radius  $\mathcal{R}$ . We scale the coordinates, momenta and the Hamiltonian  $H$  itself with the energy

$$\tilde{\mathcal{R}} = E\mathcal{R} \quad \tilde{\mathcal{P}} = E^{-1/2}\mathcal{P} \quad \tilde{H} = E^{-1}H \equiv 1. \quad (2)$$

From equation (2) it follows that the orbital angular momentum  $L$  and the action  $\Phi$ —both have the same dimensions—scale as

$$\tilde{L} = \tilde{r} \wedge \tilde{p} = \sqrt{E}\vec{r} \wedge \vec{p} = \sqrt{E}\vec{L}. \quad (3)$$

The angles and the corresponding generalized momenta are dimensionless and therefore not affected by the scaling. The scaled Hamiltonian reads

$$\tilde{H} \equiv 1 = \frac{\tilde{p}^2}{2} + \frac{\tilde{\Lambda}^2(\Omega)}{2\tilde{\mathcal{R}}^2} + \frac{C(\Omega)}{\tilde{\mathcal{R}}} \quad (4)$$

where  $\Lambda(\Omega)$  is the grand angular momentum operator, which contains the dependence upon all the momenta in the angles  $\Omega$  while  $C(\Omega)$  can be viewed as an angle-dependent generalized charge whose exact form is not important for the present context. From the structure of the Hamiltonian one can derive the following properties (see appendix A):

(i) As a function of time the hyperradius  $\mathcal{R}(t)$  has one extremum that is a minimum.  
(ii) In the limit  $E \rightarrow 0$  the dynamics for any (preserved) total angular momentum  $L$  in a two-electron atom is governed by the same effective Hamiltonian as  $L = 0$  (this follows immediately from (3)).

(iii) The angle  $\theta_{12} = 180^\circ$ , for instance, between the electrons in a two-electron atom is a fixed point of the classical equations of motion, i.e. if  $\theta_{12}(t_0) = 180^\circ$  and  $\dot{\theta}_{12}(t_0) = 0$  then  $\theta_{12}(t) = \theta_{12}(t_0)$  for all times  $t$ . It must be emphasized that this property holds only for three particles and not in the general case of  $N$  particles.

### 2.3. The $S$ -matrix for fragmentation in the limit $E \rightarrow 0$

The relevant dynamical object for scattering is the  $S$ -matrix which describes the transition from an initial state  $|i\rangle$  to a final state  $|f\rangle$ . In the momentum representation we may write

$$S_{fi}(E) = \lim_{|t| \rightarrow \infty} \int \langle f|p\rangle \langle p| \exp\left(\frac{-iHt}{\hbar}\right) |p'\rangle \langle p'|i\rangle dp' dp \quad (5)$$

where we have formally denoted the  $(3N - 3)$ -dimensional momentum vector as  $p$ . The propagator can now be expressed with Feynman's path integral

$$\langle p| \exp\left(\frac{-iHt}{\hbar}\right) |p'\rangle = \int \mathcal{D}[\bar{p}] \exp\left(\frac{i\Phi[\bar{p}]}{\hbar}\right) = \int \mathcal{D}[\bar{p}] \exp\left(\frac{i\tilde{\Phi}[\bar{p}]}{\hbar E[\bar{p}]^{1/2}}\right) \quad (6)$$

where  $\Phi[\bar{p}] = \int L dt$  is the classical action along an individual path  $\bar{p}(t)$ . The action scales with the energy of the path, according to (3), as  $\Phi[\bar{p}] = \tilde{\Phi} E[\bar{p}]^{-1/2}$ . Generally the paths contributing to the path integral (6) will have different energies  $E[\bar{p}]$  and it is not possible to identify the energy  $E$  of the  $S$ -matrix with the energy  $E[\bar{p}]$  of the paths.

For complete fragmentation, however, the final state of asymptotically free particles  $\langle p|f\rangle = \delta(p - p_f)$  forces all paths in (6) on the energy shell,  $E[\bar{p}] \equiv E$ . Hence, for any finite action  $\tilde{\Phi}$  the integrand in (6) will oscillate infinitely rapidly for  $E[\bar{p}] = E \rightarrow 0$  and on mathematical grounds we can evaluate the (path)-integral by stationary phase, i.e. with the paths that minimize the action  $\delta\Phi[\bar{p}] = 0$ . Of course, these paths are just the solutions of the classical equations of motion and the result is the same as the semiclassical limit  $\hbar \rightarrow 0$  of the Feynman path integral. This is also obvious from (6) where only the product  $\hbar E[\bar{p}]^{1/2}$  appears. The fact that the energy  $E[\bar{p}]$  of the paths for fragmentation is the energy  $E$  of the system enables us to identify the limit  $E \rightarrow 0$  with the semiclassical limit  $\hbar \rightarrow 0$  of the path integral.

### 2.4. Simplifying approximations for threshold ionization

With the results from sections 2.2 and 2.3 we can justify a considerable simplification for electron- or positron-atom scattering close to the fragmentation threshold (the atom is

treated as a core with one active electron). Using (ii) from section 2.2 we may describe the DDCs of (1) with the  $L = 0$  partial wave only. The situation seems to be similar to the familiar elastic scattering under short-range forces where a partial wave analysis shows that only  $L = 0$  survives for  $E \rightarrow 0$ . Note however, that the situation is in fact radically different for inelastic Coulomb scattering: all partial waves contribute with an *a priori* unknown weight but the dynamics for each  $L$  is determined in the limit  $E \rightarrow 0$  by the same Hamiltonian as for the  $S$ -wave. Formally, we may write (suppressing here and in the following the labels  $S$  and  $\pi$  when not explicitly needed)

$$\sigma_L(E \rightarrow 0, \epsilon, \theta_{12}, \alpha') \approx s_L \sigma_0(E, \epsilon, \theta_{12}, \alpha') \quad (7)$$

where the  $s_L$  are simple numbers and specify the relative weight of the partial cross sections  $\sigma_L$  for  $E \rightarrow 0$ . With equation (7) the DDCs of (1) becomes proportional to the  $L = 0$  partial intensity

$$\frac{d^2\sigma}{d \cos \theta_{12} d\epsilon}(E \rightarrow 0) \approx \beta' \sigma_0(E, \epsilon, \theta_{12}, \alpha') \quad (8)$$

with  $\beta' = \sum_L s_L$ .

Furthermore, with (iii) we can expect that the main contribution to the single differential cross section (i.e. integrated over  $\theta_{12}$ ) comes from the fixed point at  $\theta_{12} = 180^\circ$ . With this final approximation the single differential cross section close to threshold reduces to

$$\frac{d\sigma(E)}{d\epsilon} \approx \beta \sigma_0(E, \epsilon, \theta_{12} = 180^\circ, \alpha'). \quad (9)$$

Hence, leaving only the overall normalization  $\beta$  undetermined, the classical problem necessary to solve for a semiclassical approximation of (9) has been reduced from 12 phase space variables to 4, the two electron-nucleus distances  $r_i$  and the conjugate momenta  $p_i$ .

### 3. The semiclassical $S$ -matrix for the $L = 0$ partial wave

#### 3.1. The collinear Hamiltonian and its implications for the scattering amplitude

The scattering for the  $L = 0$  partial wave at  $\theta_{12} = 180^\circ$  may be regarded as an approximation to the total cross section justified for  $E \rightarrow 0$  within the semiclassical  $S$ -matrix approach following the steps from (1) to (9). Alternatively one might look at it as a model for scattering under the Hamiltonian

$$H = \frac{p_1^2}{2m_{AC}} + \frac{p_2^2}{2m_{BC}} - \frac{p_1 p_2}{m_C} - \frac{1}{r_1} - \frac{1}{r_2} + \frac{1}{r_1 + r_2} \quad (10)$$

in atomic units ( $e = m_e = \hbar = 1$ ). Since  $\hbar$  plays a crucial role in the semiclassical limit we will write  $\hbar$  explicitly in the important equations. The mass indices indicate the reduced masses  $m_{\alpha\beta} = m_\alpha m_\beta / (m_\alpha + m_\beta)$  between the particles  $\alpha$  and  $\beta$ . The particles A and B have the same polarity and particle C has opposite polarity, so that  $r_1 = r_{AC}$  and  $r_2 = r_{BC}$ . In the case of electron-atom scattering the nucleus would be the third particle with  $1/m_C = 0$ . For positron-atom scattering the electron is particle C with  $1/m_C = 1$ , and the nucleus is particle B with  $m_{BC} = 1$  and  $m_{AC} = \frac{1}{2}$ . In the past the Hamiltonian (10) was studied quantum mechanically as well as classically (Blümel and Reinhardt 1991, Kim and Ezra 1991). We will give a self-consistent semiclassical scattering amplitude  $S_{s,\epsilon'}$  for the Hamiltonian (10) and ultimately with this result describe the true physical situation close to threshold in the context of (9). Quantum mechanically, even for a partial cross section at  $\theta_{12} = 180^\circ$ , it is necessary to treat the angle  $\theta_{12}$  as a dynamical variable for the

collision. Semiclassically, however, because of the fixed point at  $\theta_{12} = 180^\circ$  (see (ii)), one can treat  $\theta_{12}$  as a parameter throughout the dynamical calculation, i.e. one can start from the *collinear* Hamiltonian (10) and interpret the result later as  $\sigma_0$  in (9). There is, however, a subtle problem in the transition from the quantum mechanical to the semiclassical treatment of (10). The variables  $r_i$  are not Cartesian coordinates but radii in spherical coordinates. It is cumbersome to switch in the semiclassical path integral representation from Cartesian coordinates to any set of curved coordinates. This will introduce additional terms in the effective Lagrangian to be used in the propagator (see Gutzwiller 1990, p 202). For the special case of spherical coordinates an additional centrifugal potential which acts like an artificial angular momentum appears in the Lagrangian. This term, known as the 'Langer modification', has been investigated recently in the context of the semiclassical propagator for a Coulomb potential by Manning and Ezra (1994). In the present treatment of threshold ionization we have not included the curvature correction for the same reason that we have used the  $L = 0$  partial wave exclusively (see (ii) in section 2.2).

The formulation of the cross section is now straightforward. Since for each particle there has only one dimension left, the cross section with the dimension of an area in  $D = 3$  reduces in  $D = 1$  to a probability, directly proportional to the square modulus of the symmetrized  $S$ -matrix, semiclassically given by

$$S_{\epsilon, \epsilon'}(E) = \sum_j \sqrt{\mathcal{P}_j(\epsilon, \epsilon')} \exp \left[ \frac{i\Phi_j}{\hbar} - \frac{i\nu_j\pi}{2} \right]. \tag{11a}$$

The weight of the  $j$ th trajectory is determined by its probability

$$\mathcal{P}_j(\epsilon, \epsilon') = \frac{1}{R} \left| \frac{\partial \epsilon}{\partial r'_j} \right|_{\epsilon'}^{-1} \tag{11b}$$

where  $R$  is the normalization constant resulting from the preservation of classical probability and  $r'_j$  is the initial position of the projectile on the  $j$ th trajectory. The sum runs over all classical trajectories  $j$  that take the projectile from energy  $\epsilon'$  to  $\epsilon$  during the collision. Each trajectory accumulates a phase, which is defined by the classical action  $\Phi_j(\epsilon, \epsilon') = \int q_1 dp_1 + \int q_2 dp_2$  and a contribution of  $\nu_j\pi/2$  from caustics along the trajectory (Gutzwiller 1990).

### 3.2. Connection with Miller's classical $S$ -matrix

The form of the semiclassical  $S$ -matrix (11a) is similar to Miller's 'classical  $S$ -matrix' (Miller 1974) for transition probabilities between an initial bound state with quantum number  $n'$  to a final state with quantum number  $n$ . In this case the  $S$ -matrix reads (Miller 1974, equation (3.30))

$$S_{n, n'}(E) = \sum_{cl. traj.} i \left[ -2\pi i\hbar \left( \frac{\partial n}{\partial \bar{q}'} \right)_{n'} \right]^{-1/2} \exp \left[ \frac{i\Phi(n, n'; E)}{\hbar} - \frac{i\nu\pi}{2} \right]. \tag{12}$$

We have added the sum over the trajectories and the phase  $\nu$  due to the Maslov indices not explicitly mentioned by Miller. Furthermore, we have adopted Miller's notation to our situation by mapping the multidimensional quantum number vector of the initial state into our single quantum number for the one-dimensional bound state  $\vec{n}_1 \rightarrow n'$  and similarly for the final state  $\vec{n}_2 \rightarrow n$ . The phase space variables  $(n, \bar{q})$  represent a pair of conjugate action-angle variables where the classical action is taken at its quantized integer value  $n$ .

This 'quantum number function'  $n = n(\epsilon)$  is classically continuous and with its help we can rewrite  $\mathcal{P}(\epsilon, \epsilon')$  from (11b) (we suppress the index  $j$  for a specific trajectory) as

$$\mathcal{P}(\epsilon, \epsilon') \equiv \left. \frac{\partial P}{\partial \epsilon} \right|_{\epsilon'} = \left. \frac{\partial P}{\partial n} \right|_{\epsilon'} \frac{\partial n}{\partial \epsilon} \equiv \mathcal{P}(n, \epsilon') \frac{\partial n}{\partial \epsilon}. \quad (13)$$

The most important modification, however, concerns the initial state which we would like to describe with the asymptotic position  $r'$  of the projectile and not the classical angular variable  $\bar{q}$  of the target electron. The connection between these two variables in the asymptotic limit before the collision was already given by Miller (1974, equation (3.31))

$$\bar{q}' = q' - \frac{\partial(E - \epsilon')}{\partial n'} \frac{r'}{p'} \quad (14)$$

where  $p'$  is the momentum of the projectile before the collision and  $E - \epsilon' = -(2n'^2\hbar^2)^{-1}$  is the hydrogenic bound state energy. Then

$$\frac{\partial(E - \epsilon')}{\partial n'} = \frac{1}{n'^3\hbar^2} = -\hbar(2\epsilon' - 2E)^{3/2} \quad (15)$$

so that

$$\frac{\partial \bar{q}'}{\partial r'} = \hbar \frac{(2\epsilon' - 2E)^{3/2}}{p'}. \quad (16)$$

With the results (13)–(16) we can now evaluate the chain of derivatives

$$\left. \frac{\partial \bar{q}'}{\partial n} \right|_{n'} = \left. \frac{\partial \bar{q}'}{\partial r'} \right|_{\epsilon'} \frac{\partial r'}{\partial \epsilon} \left. \frac{\partial \epsilon}{\partial n} \right|_{\epsilon'}. \quad (17)$$

The action  $\Phi$  of the  $S$ -matrix is independent of the coordinates. Hence, equation (11a) agrees with (12) under the normalization

$$R(\epsilon', E) = 2\pi p' (2\epsilon' - 2E)^{-3/2}. \quad (18)$$

In terms of the classical trajectories for the electrons the normalization (18) has a direct physical interpretation which will be discussed in the next section.

### 3.3. The choice of initial conditions

Although unfamiliar it is completely equivalent to the conventional procedure to take the radial distance  $r'$  of the projectile from the scattering centre as an 'impact parameter'. The usual initial conditions for the scattering may be formulated as follows. The bound electron moves on a Kepler ellipse without eccentricity and with binding energy  $E_B = \frac{1}{2}$  au (we describe a 1s ground-state electron of hydrogen). The free electron has an energy of  $\epsilon' = E + E_B$  and its trajectory is started at some position  $r'_0$  sufficiently far away from the scattering centre (the nucleus) to define an asymptotic state. The only free parameter to vary is the phase  $\phi_0$  of the electron on the bound orbit. Since only positions and momenta of projectile and target electron *relative* to each other are relevant to specify an asymptotic scattering state we can formulate an equivalent but numerically more convenient set of initial conditions: the trajectory of the bound electron is always started at the outer turning point of the ellipse so that the momentum of the target electron is zero. The initial distance of the projectile from the nucleus is taken to be  $r'_0 + r'$  where  $r'_0$  is fixed at some arbitrary distance large enough so that the result is independent of  $r'_0$  (we have taken 1000 au). Instead of the phase  $\phi_0$  we vary  $r'$  over the length that the projectile travels during the time the target electron needs to complete a full period of motion. Thus,  $r'$  serves as a generalized 'impact parameter' in our

approach. This choice of initial conditions is numerically more convenient because the Coulomb singularity, i.e. the initial condition where the trajectory of the target electron is at its inner turning point (with infinite momentum at the position of the nucleus), can be avoided.

### 3.4. Relation to previous classical work

The approach described here utilizes only information from classical orbits which are also the basis of classical trajectory work on electron-hydrogen, electron-He<sup>+</sup> and positron-hydrogen scattering (Abrines and Percival 1966, Boesten L G J *et al* 1976, Dimitrijevic and Grujić 1983, Read 1984, Gailitis 1986, Wetmore and Olson 1986, Gu and Yuan 1993, for reviews see Rau 1984, Read 1984a and Grujić 1986). There are some minor differences concerning technical details like the regularization of the Coulomb singularities which is described well by Gaspard and Rice (1993) for the electron-hydrogen system. We use essentially the same procedure, the difference is that instead of the new time differential  $d\tau = dt/(r_1 r_2)$  we take  $d\tau = dt/(r_1 + r_2)$  which is more appropriate for the scattering application. The regularization has the pleasant side effect that integration of the trajectories to extremely large distances  $r_i$  is possible with a moderate number of time steps  $\Delta\tau$ . The feature is not only pleasant but crucial for a converged ionization probability calculation for  $E \rightarrow 0$ . In this limit only at very large distances can it be determined whether slow electrons belong ultimately to a highly excited Rydberg orbit or if they are really continuum electrons.

The major difference to previous classical work, however, lies in the theoretical formulation of the scattering problem. Within the framework of a semiclassical  $S$ -matrix it is possible to provide a complex scattering *amplitude*. With equation (11a) we can formulate a differential cross section from a specified initial state including all sorts of interference effects from different classical paths. Of course, the scattering amplitude is an approximation. However, it has invaluable conceptual advantages, in particular, for ionization under long-range (Coulomb) potentials. The difficult question of a final state for three or more charged particles in the continuum does not arise since the boundary conditions appear naturally for the semiclassical  $S$ -matrix through the properties of the classical trajectories. From each trajectory only the final momentum of the projectile must be extracted to determine if the trajectory contributes to fragmentation, excitation or (classical) exchange. This will become much clearer through the following example.

Moreover, specialized to the three-body Coulomb fragmentation, the reduction to the 'collinear problem' of two degrees of freedom, often thought of as a model assumption, can be justified as a reasonable approximation for energies close to threshold within the  $S$ -matrix approach as formulated above. However, what 'close' means quantitatively cannot be determined within the approximation. As we will see in section 5 the comparison with the experiment suggests a range of validity of the collinear semiclassical  $S$ -matrix up to 8–10 eV above threshold for ionization of hydrogen by electron impact. With the scaling law to be described in section 6 the corresponding range of validity for other targets is easily deduced and in agreement with the experimental cross sections. Since the collinear  $S$ -matrix remains valid well above the threshold  $E = 0$  it is possible to determine threshold properties and even the range of excess energies for typical threshold behaviour within the present approach (Rost 1994).

#### 4. Positron-hydrogen scattering close to the fragmentation threshold

##### 4.1. The classical deflection function

As can be seen from (11b) the crucial quantity for the S-matrix is the classical deflection function,  $\epsilon(r')$ . A more familiar example for a deflection function (which is introduced, for example, in Brink (1985) or Jung (1986)) is  $\Theta(b)$  in Rutherford scattering where  $\Theta$  is the scattering angle and  $b$  is the impact parameter. As already mentioned above,  $r'$  plays the role of the impact parameter and the final energy  $\epsilon$  of the projectile is the final state observable which corresponds in Rutherford scattering to the scattering angle  $\Theta$ .

The present deflection function  $\epsilon(r')$ , shown in figure 1, reveals three intervals  $I(i)$  of initial conditions leading to physically distinct final states. For  $r' \in I(1)$  positronium is formed in a classical exchange reaction indicated by the negative energy  $\epsilon < 0$ . The positronium energy  $\epsilon$  is defined relative to the energy of the centre of mass between the proton and the positronium. Fragmentation into three free particles for  $r' \in I(2)$  and excitation with  $r' \in I(3)$  both create a free positron whose kinetic energy defines  $\epsilon$  relative to the proton which is at rest. The necessary frame transformation leads to a piecewise continuous deflection function. It has a 'gap' at the border between  $I(1)$  and  $I(2)$  where the coordinates are changed. The reason is that in the rest frame of the proton positronium is formed at a positron kinetic energy of  $\epsilon = E/2$ . Hence, fragmentation only occurs with final positron energies  $E/2 < \epsilon < E$ . Finally, with  $r' \in I(3)$  and  $\epsilon > E$ , excitation occurs with the electron remaining bound after the collision.

Remarkably, the deflection function  $\epsilon(r')$  is *monotonic*: it has only one intersection with a horizontal line at  $\epsilon$  indicating the correct initial condition  $r'$ . In other words to each differential cross section with a final projectile energy  $\epsilon$  only a *single* trajectory contributes. This property can be understood from (i) in section 3.2 where it was shown that each trajectory is uniquely described by the value for its minimum hyperradius  $\mathcal{R}$ . It is a general property of the classical dynamics for particles interacting through Coulomb forces irrespective of the individual charges.

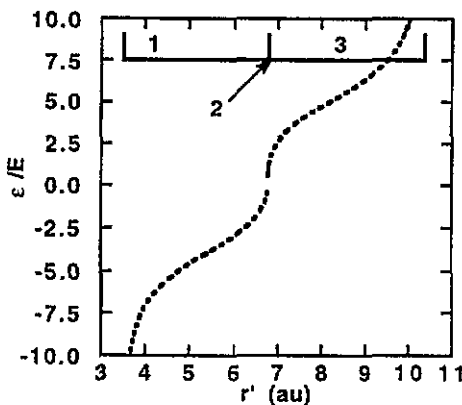


Figure 1. The final energy  $\epsilon > 0$  of the positron as a function of its initial position  $1000 \text{ au} + r'$  at a total energy of  $E = 0.1 \text{ au}$ . Positronium with energy  $\epsilon$  is formed for  $\epsilon < 0$ . The intervals  $I(i)$ ,  $i = 1, 2, 3$  of initial conditions lead to different physical processes, positronium formation, fragmentation and excitation, see text.

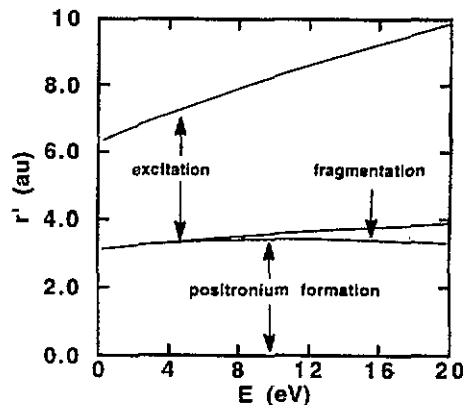


Figure 2. The initial values  $r'$  leading to different inelastic scattering events as a function of total energy.

4.2. Energy dependence of the total cross section

With only one term remaining in the sum of (11a) the semiclassical result collapses to the classical cross section (Rost and Heller 1994) without any effects from the phase factor of (11a) to give

$$P_{\epsilon, \epsilon'}(E) = \mathcal{P}(\epsilon, \epsilon') \equiv \frac{1}{R} \left| \frac{\partial r'}{\partial \epsilon} \right|_{\epsilon'} \quad (19)$$

The total cross section is then simply proportional to the intervals of  $r'$  for which a certain process, for instance fragmentation, happens:

$$P_{frag}(E) = \frac{1}{R} \int_0^E \left| \frac{\partial r'}{\partial \epsilon} \right|_{\epsilon'} d\epsilon = \frac{1}{R} \int_{r' \in I(2)} dr' = \frac{\Delta r'(2)}{R} \quad (20a)$$

The normalization is given by the sum of all processes that can happen,

$$R = \sum_{i=1}^3 \Delta r'(i) \quad (20b)$$

The intervals  $\Delta r'(i)$  can be read off directly from figure 2. The relative probabilities  $P_i(E) = \Delta r'(i)/R$  are shown in figure 3. Excitation and positronium formation are the dominant processes close to threshold while the cross section for fragmentation is very small. The fragmentation cross section initially follows the power law  $\sigma(E) \propto E^{2.65}$  derived by Klar (1981b) from the Wannier threshold theory in the limit  $E \rightarrow 0$  (see figure 4). For higher excess energy the calculated cross section is flatter than the Wannier threshold prediction. The same tendency is found in electron-hydrogen scattering to be discussed in section 5.

The easiest way to obtain the fragmentation cross section experimentally in electron-atom scattering is to count the ions in the exit channel. The fragmentation of the positron-hydrogen or, in general, a positron-atom system near threshold is more complicated to observe, since in the ion signal fragmentation must be discriminated against positronium formation which also produces ions. Furthermore, due to the large exponent  $\alpha = 2.65$  the fragmentation cross section is much smaller for positron impact than it is for electron impact ( $\alpha = 1.127$ ) resulting in poor statistics in the experiment. However, our results contain one

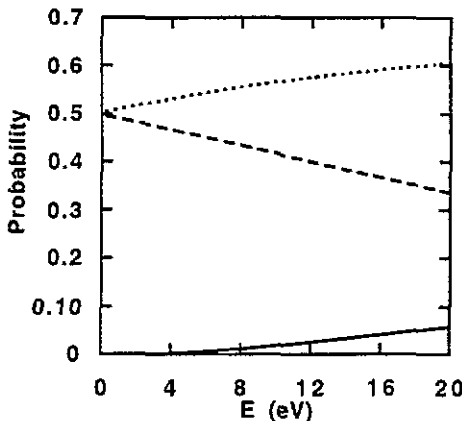


Figure 3. Relative probabilities for fragmentation (full curve), excitation (dotted curve) and positronium formation (broken curve).

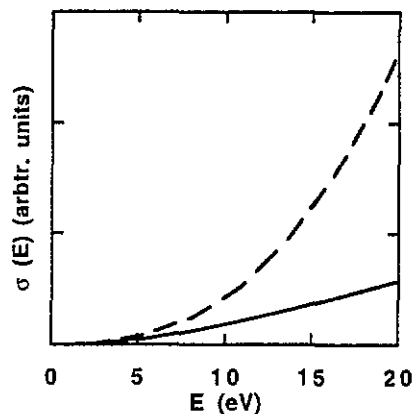


Figure 4. The fragmentation probability as a function of excess energy. The broken curve represents a fit with the function  $\beta E^{2.65}$ .

positive aspect of threshold fragmentation by positron impact: the threshold regime extends to higher excess energies than in electron impact ionization. Hence, it is possible to probe the threshold properties experimentally at higher energies where the yield is already better. Hopefully experiments will be performed in the near future (Weber and Raith 1994).

Our analysis has revealed that the fragmentation of hydrogen by positron impact close to threshold is essentially a classical process since no interferences from different classical paths occur. Hence, the classical calculation should give the same result. Surprisingly, Wetmore and Olson (1986) extract from their classical-trajectory Monte Carlo (CTMC) data a threshold exponent of  $\alpha \approx 3$ . However, only data higher than 5 eV excess energy were used for the determination of the exponent due to very poor statistics for the cross section closer to threshold. (In this sense the CTMC calculation must fight the same difficulties as the experiment.) Wetmore and Olson conclude for these reasons that the CTMC exponent might not be reliable.

#### 4.3. A simple derivation of the semiclassical $S$ -matrix

Before we continue with electron impact scattering we will demonstrate briefly how the scattering amplitude (11a) can be derived in a very simple manner with the insight we have gained in the present section. From the initial conditions as described at the end of the last section we know that the length  $R$  representing the normalization is the distance that the (asymptotically free) projectile travels during a complete cycle  $T$  on the Kepler ellipse of the bound electron,  $R = Tp'$ . This is also the direct outcome of (20b) since the deflection function  $\epsilon(r')$  is periodic in  $r'$  with the period  $R$  triggered by the period of the bound motion according to  $R = Tp'$ . The classical period  $T$  for a bound electron is given (in atomic units) by  $T = 2\pi(2\epsilon' - 2E)^{-3/2}$  (Goldstein 1980, p 100) which leads with the momentum  $p'$  of the projectile to (18). The normalization guarantees that the classical probability to find the projectile after the collision is (still) unity. (Semiclassically, the  $S$ -matrix preserves unitarity only to the order of  $\hbar$ ).

Now we have derived the functional dependence of the normalization  $R(E, \epsilon')$  in a very simple way without referring to Miller's  $S$ -matrix†. We can complete this shortcut for the derivation of the semiclassical  $S$ -matrix with the following argument. It is clear from energy conservation and the total dimensionality of the problem (four phase space variables) that the classical probability  $\mathcal{P}$  is a simple derivative of an appropriate *one-dimensional* deflection function. Any final and initial parameter suitable to characterize the dynamics can be chosen and their mutual dependence creates a deflection function. The normalization will be different for each choice of variables but the scattering amplitude will always be the same. Thus, the only non-trivial quantity is the normalization which we have just determined.

## 5. Electron impact ionization of hydrogen close to the threshold

### 5.1. The classical cross section

Compared to positron-impact scattering we have to deal with one more complication, the symmetrization of the indistinguishable electrons. However, in a first step we may ignore the Pauli principle and calculate the classical scattering probability. The deflection function  $\epsilon(r')$  in figure 5 has exactly the same structure as in positron-hydrogen scattering, in

† The derivation of the normalization does not hinge upon the monotony of the deflection function, see for instance Rost (1994c).

particular it is monotonic so that there is again only the contribution of one trajectory to the unsymmetrized  $S$ -matrix. The intervals of initial conditions describe the same physical processes as in figure 1, namely  $r' \in I(1)$  represent classical exchange trajectories,  $r' \in I(2)$  stands for ionization (fragmentation) and  $r' \in I(3)$  leads to excitation. Since the energy of the bound electron in  $I(1)$  as well as the kinetic energy of the free electron in  $I(3)$  are defined relative to the same centre of mass, the proton which is at rest, there is no frame transformation necessary. Hence, unlike in the positron-hydrogen case, there is no 'gap' in the deflection function. In analogy to (20a) we can define the classical cross section for ionization in electron-hydrogen scattering by

$$P_{cl}(E) = \int_0^E \mathcal{P}(\epsilon, \epsilon') d\epsilon = \frac{1}{R} \int_0^E \left| \frac{\partial r'}{\partial \epsilon} \right|_{\epsilon'} d\epsilon = \frac{\Delta r'(2)}{R} \tag{21}$$

which behaves for  $E \rightarrow 0$  like  $P_{cl} \propto E^{1.127}$  (see figure 6) as predicted analytically by Wannier (1953). How does the result change if the Pauli principle is employed?

### 5.2. The differential cross section

The scattering amplitude must now be symmetrized with respect to the identical electrons leading to a singlet (+) and a triplet (-) partial cross section

$$\begin{aligned} {}^1S^e : \frac{d\sigma^s}{d\epsilon} &\equiv P_{\epsilon, \epsilon'}^+(E) = |S_{\epsilon, \epsilon'}(E) + S_{E-\epsilon, \epsilon'}(E)|^2 \\ {}^3S^e : \frac{d\sigma^s}{d\epsilon} &\equiv P_{\epsilon, \epsilon'}^-(E) = |S_{\epsilon, \epsilon'}(E) - S_{E-\epsilon, \epsilon'}(E)|^2 \end{aligned} \tag{22}$$

with the  $S$ -matrix element  $S_{\epsilon, \epsilon'}(E)$  as in (11a). Since quantum mechanics is linear in the amplitude (the wavefunction) it is legitimate to take a symmetry into account a posteriori as in (22). In fact this is the standard quantum mechanical procedure in scattering theory (compare e.g. Taylor 1972, chapter 22).

In the present context special circumstances help to simplify (22). It is convenient to introduce a scaled energy variable  $x = \epsilon/E - 1/2$  so that the electron exchange is given by inversion,  $x \rightarrow -x$ . Keeping in mind that only one trajectory contributes to  $S_{x, x'}(E)$  the

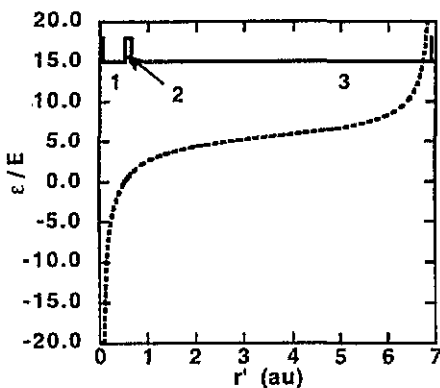


Figure 5. Classical deflection function for the final energy  $\epsilon$  of the projectile electron as a function of its initial position  $1000 \text{ au} + r'$  at a total energy of  $E = 0.1 \text{ au}$ . The intervals  $I(i), i = 1, 2, 3$  mark different physical processes, see the text.

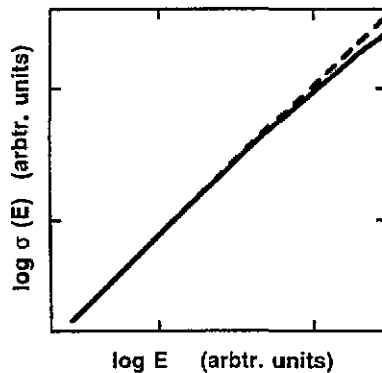


Figure 6. The total cross section according to Wannier (broken curve) and from (21).

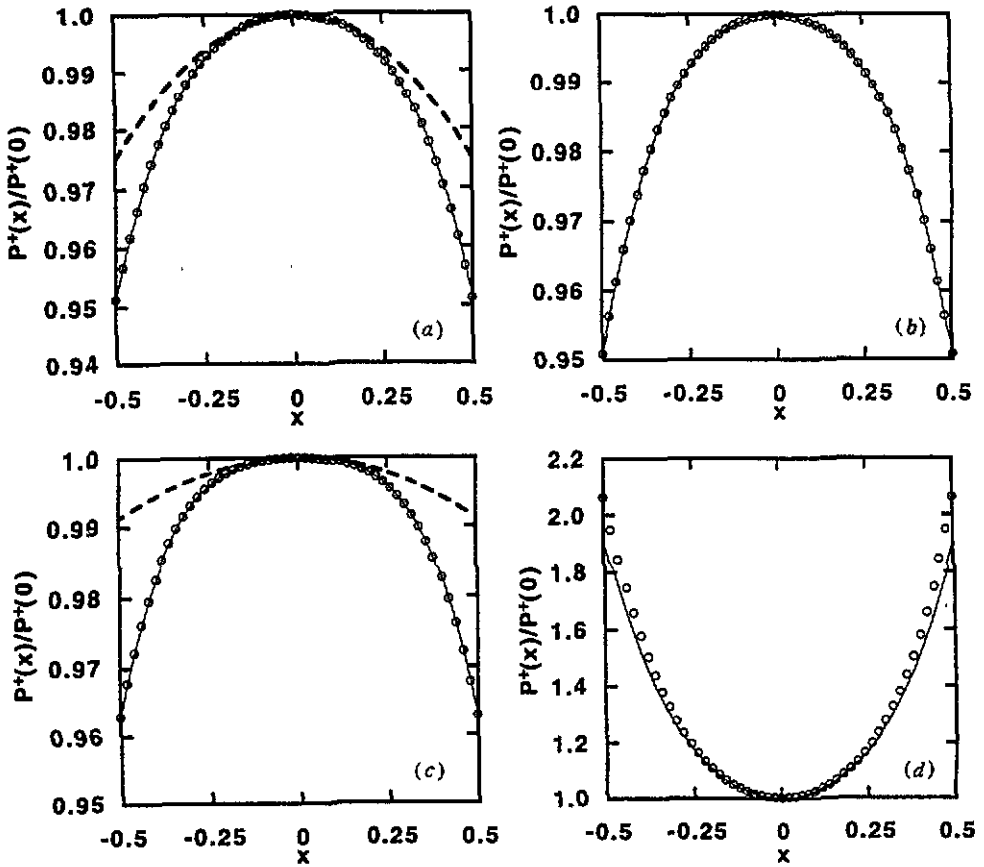


Figure 7. The energy sharing probability  $P^+(x)$  normalized to the value at  $x = 0$  for various excess energies, (a)  $E = 10^{-3}$  au, (b)  $E = 10^{-2}$  au, (c)  $E = 10^{-1}$  au and (d)  $E = 1$  au. The exact values are denoted by circles, the full curve and the broken curve correspond to approximations, see the text.

symmetrized probabilities (22) are now constructed from the coherent sum of two classical paths which could show an interference pattern. However, the action is exactly symmetric under electron exchange  $\Phi(x, x') = \Phi(-x, x')$ . This property originates in the Coulomb interaction only in so far as it has been possible to reduce the relevant phase space to four dimensions which is the true reason for the symmetric action (see the proof in appendix B). We now have the simple differential probabilities

$$P_{x,x'}^\pm(E) = \left( \sqrt{\mathcal{P}(x, x')} \pm \sqrt{\mathcal{P}(-x, x')} \right)^2. \quad (23)$$

Normalized to  $P_{0x'}^+$  they are shown in figure 7 for energies spanning three orders of magnitude from  $E = 10^{-3}$  to 1 au. In the singlet configuration at threshold there is a preference of about 5% for equal energy sharing. This threshold energy sharing was also obtained by Read (1984) and Gailitis (1986) in classical trajectory calculations without a physical initial state. Our present findings, with a well defined initial state, together with these previous results confirm that certain properties of threshold ionization are independent of the initial state as already predicted by Wannier (1953). For more details see Rost (1994c). However, only in the limit  $E \rightarrow 0$  is the energy distribution universal with a 5%

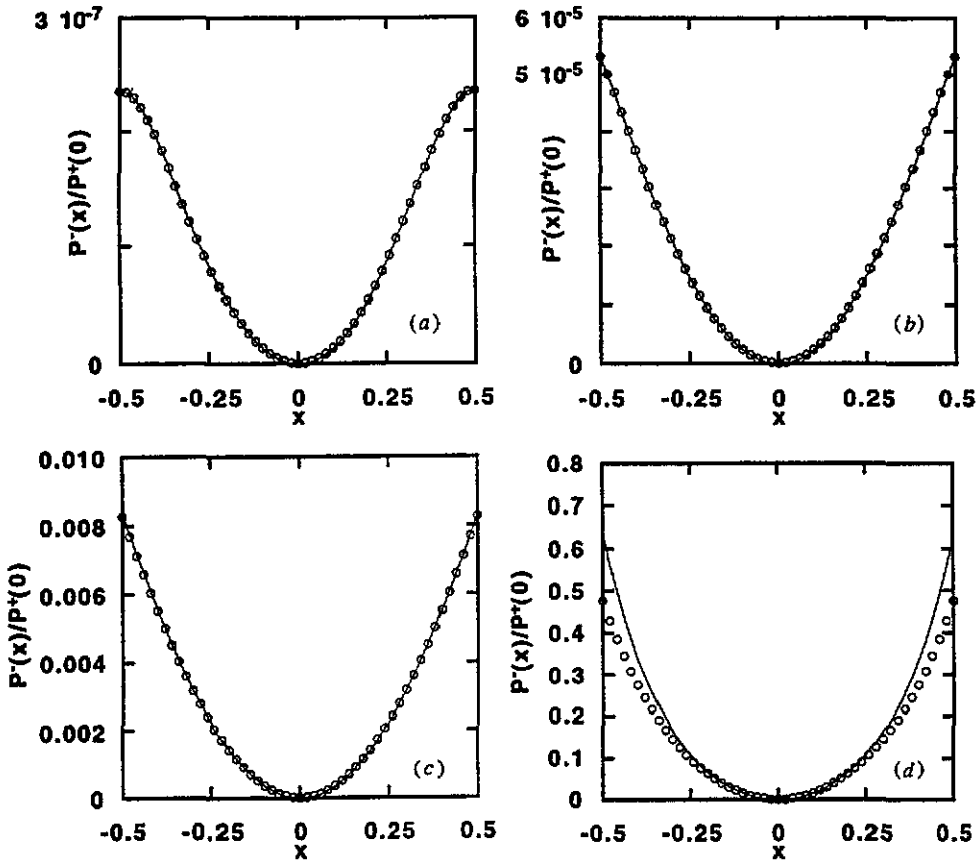


Figure 8. Same as figure 7, but for the  $P^-(x)$  probability, normalized to  $P^+(0)$ .

preference for equal energy sharing. As described in Rost (1994) this preference decreases towards a 'transition region' around 3 eV excess energy where the energy distribution is flat within 1%. For higher energies a preferred unequal energy sharing is approached (with a fast projectile electron and a slow target electron). In the  $^3S^e$  symmetry there is no transition since equal energy sharing is not allowed. Hence, the shape of the cross section changes only slightly for different excess energies (figure 8). The ratio of triplet to singlet probability is reflected by  $P_x^-/P_0^+$  which demonstrates that the triplet probability is orders of magnitude smaller relative to the singlet probability for small excess energies. At  $E = 1$  au both probabilities have the same order of magnitude (compare figure 7(d) with 8(d)). The behaviour can be understood analytically from a perturbation expansion of the triple collision manifold, a task which is beyond the scope of the present paper. However, we use a result from this analysis to interpret figures 7 and 8.

### 5.3. Analytical interpretation of the differential scattering cross section

The unsymmetrized scattering amplitude  $\mathcal{P}(x)$  can be represented as a sum of two functions  $P_g(x)$  and  $P_u(x)$  which are symmetric and antisymmetric under electron exchange. These two functions scale differently with the total energy, namely (Rost 1994d)

$$P_g(x, x', E) \propto E^\alpha \quad P_u(x, x', E) \propto E^{2\alpha} \quad (24)$$

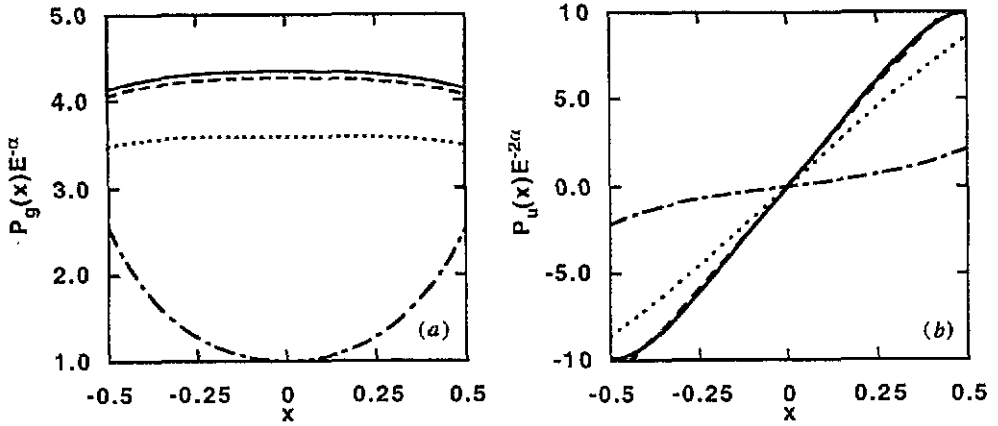


Figure 9. The classical probabilities, (a)  $P_g(x)$ , and (b)  $P_u(x)$  as defined in the text and scaled according to their behaviour with the total energy for  $E = 10^{-3}$  au (full curve),  $E = 10^{-2}$  au (broken curve),  $E = 10^{-1}$  au (dotted curve) and  $E = 1$  au (chain curve).

where  $\alpha = 1.127$  is the Wannier exponent (Wannier 1953). The reason for the scaling can be found from an analysis of the triple collision manifold (TCM) which is responsible for the ionization dynamics in the limit  $E \rightarrow 0$  (Eckhardt 1991). Essentially, each contact of a trajectory with the TCM leads to a factor  $E^\alpha$  in the probability for this trajectory. For trajectories contributing to  $P_g$  one contact is sufficient while for the antisymmetric probabilities two contacts with the TCM are necessary. This explains the scaling (24) which is demonstrated in figure 9 for an energy range spanning the same three orders of magnitude,  $10^{-3} \leq E \leq 1$  au as in the previous figures. While the total energy dependence follows (24) very well, the dependence of  $P_g(x)$  and  $P_u(x)$  on  $x$  changes appreciably from  $10^{-3}$  au to 1 au excess energy.

As an immediate consequence of (24) we can expand the mixed term in the singlet and triplet probabilities  $P^\pm$  from (23) according to

$$P^+(x, x', E) \approx 2P_g(x) - \frac{P_u(x)^2}{2P_g(x)} \propto E^\alpha$$

$$P^-(x, x', E) \approx \frac{P_u(x)^2}{2P_g(x)} \propto E^{3\alpha}.$$
(25)

The approximation (25), shown in figures 7 and 8 with open circles, is excellent for small excess energies and even for  $E = 1$  au is still reasonable. From equation (25) it follows that  $P^+/P^- \approx E^{-2\alpha}$  which for  $E = \frac{1}{10}$  au is still a factor of 100.

With regard to the question of semiclassical corrections to the classical result close to threshold our analysis shows that even the triplet cross section is classical in the sense that no  $\hbar$  dependence occurs. Due to the symmetry of the action  $\Phi(x)$  under electron exchange, classical probabilities in the form of (23) are sufficient to describe the symmetrized cross sections. The result might prove interesting for the justification of purely classical trajectory methods such as the CTMC. With the classical probabilities obtained by these methods symmetrized cross sections could be constructed according to (23).

Most Wannier-like threshold approaches use a quadratic approximation about the Wannier saddle ( $x = 0, \theta_{12} = 180^\circ$ ). In this context it is interesting to note that the energy sharing distribution  $P^\pm(x)$  can only be represented by a function quadratic in  $x$  in a very limited region around  $x = 0$  (see the broken curves in figures 7(a) and (c)).

The necessity to go beyond the quadratic approximation has also been emphasized recently by Kazansky and Ostrovsky (1994). Another necessary extension of the Wannier theory towards reliable differential observables like the energy sharing probability is a realistic description of the initial state. Without invoking the Wannier picture the present approach satisfies both criteria. Hence, the transition from the threshold behaviour manifested in preferred equal energy sharing to the preference for unequal energy sharing characteristic for higher excess energies could be demonstrated here and awaits experimental confirmation.

5.4. The total cross section

Formally the total cross section for a given symmetry is obtained by integration of (23)

$$P^\pm(E) = \int_0^{\frac{1}{2}} P_{x,x'}^\pm(E) dx. \tag{26}$$

As expected from the energy scaling (24) the singlet cross section for  $E \rightarrow 0$  follows the Wannier power law  $P^+(E) \propto E^{1.127}$  (broken curve in figure 6) and the triplet cross section behaves as  $P^-(E) \propto E^{3.381}$ . More interestingly, the symmetrized cross section  $P^+(E)$  lies very close to the purely classical total cross section (21). This follows from (25) since

$$P^+(E) \approx \int_0^{\frac{1}{2}} 2P_g(x) dx = \int_0^{\frac{1}{2}} (P(x) + P(-x)) dx = 2P_{cl}(E). \tag{27}$$

Thus, the Pauli principle mainly has the effect of doubling the classical cross section for  $^1S$  symmetry as can be expected for perfect constructive interference. Based on the underlying classical trajectories we can interpret the  $^3S$  cross section with the semiclassical  $S$ -matrix as a destructive interference effect between the two classical paths whose contribution to the scattering amplitude must be summed coherently.

In the ‘classical’ electron impact ionization experiment of McGowan and Clarke (1968) the total cross section has been measured from 0 to 8 eV excess energy. It is shown together with the present result of semiclassical  $S$ -matrix theory in figure 10. Only the overall normalization was matched at some arbitrary energy (5.82 eV).

The good agreement of the theoretical curve with the experimental data justifies *a posteriori* our approximations, first of all the semiclassical approach, and within this approach the restriction to the  $L = 0$  contribution and to the classical fixed point at  $\theta_{12} = 180^\circ$ . Still, the theoretical curve must be normalized to the data at one point since

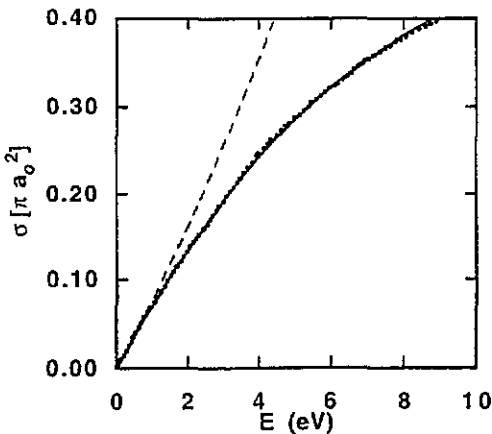


Figure 10. The total ionization cross section for electron impact on H(1s). The experimental data points are taken from McGowan and Clarke (1968). The calculated cross section (full curve) has been normalized to the experimental data at 5.84 eV. The broken curve is the Wannier cross section  $\sigma(E) = \beta E^{1.127}$ .

under the present approximations it is not possible to predict an absolute cross section. However, our inclusion of the initial state determines the energy scale which is in most threshold theories another fit parameter. Furthermore, there is no principal obstacle to calculating an absolute cross section with the semiclassical  $S$ -matrix in the future. For the time being it seems to be more interesting to see how far the simplified picture, as presented here, can describe reality. Of course, most of the experiments have been performed with targets different from atomic hydrogen. Hence, in the next section we will derive a semiempirical extension of the hydrogen theory to describe general electron-atom threshold ionization.

## 6. Electron impact ionization of atoms close to threshold

The considerable experimental material that has been accumulated over the years involves valence-shell as well as inner-shell ionization near threshold. We will show that both processes, as far as they are not influenced by core excitations, can be described like the hydrogen ionization. Similar arguments apply to positron-atom scattering. However, here the experimental material is scarce and, moreover, it is difficult to separate (experimentally) fragmentation from positronium formation. Hence, we will only discuss electron-atom scattering in the following.

### 6.1. The influence of the initial state on threshold ionization

From the Wannier theory one can deduce that the dynamical aspects of ionization near threshold are a final state property. This statement refers to observables whose properties are induced by the triple collision manifold (Eckhardt 1991, Rost 1994d), for instance the energy dependence of the total cross section, the energy sharing between the continuum electrons and the distribution in the interelectronic angle  $\theta_{12}$ . As far as the present  $S$ -matrix approach covers these observables, our results confirm the statement (see sections 5.2 and 5.4).

For our present purpose we need to ask how does the initial state influence the ionization yield for finite excess energies? We expect the universality of the threshold phenomena to persist to some extent also for finite excess energies and assume in the following empirical ansatz that the initial state determines only the energy scale  $\rho_A$  of the ionization cross section. Together with the scaling  $\beta_A$  of the absolute cross section we now have two parameters to adapt the otherwise universal threshold ionization yield to the specific targets. The cross section for threshold ionization of atom  $A$  in its specified initial state (this includes inner-shell ionization) reads then in terms of the hydrogen cross section  $\sigma_H$

$$\sigma_A(E) = \beta_A \sigma_H(\rho_A E). \quad (28)$$

Figure 11 shows ionization cross sections of valence shell electrons for He(1s), Na(3s) and, as already discussed, H(1s). In addition, three inner-shell ionization cross sections are shown, namely Ne(1s), Ar(1s) and Xe(2p). The full curves correspond to (28) with suitable scaling parameters  $\beta_A$  and  $\rho_A$ . As can be seen the agreement is generally good despite the great variation of the ionization potential from around 5 eV for Na to nearly 5 keV for Xe.

### 6.2. The energy scaling as a function of the ionization potential

We may go one step further and parametrize the energy scaling factor with the respective ionization potentials  $I_A$  of the target electrons. On a logarithmic scale the function

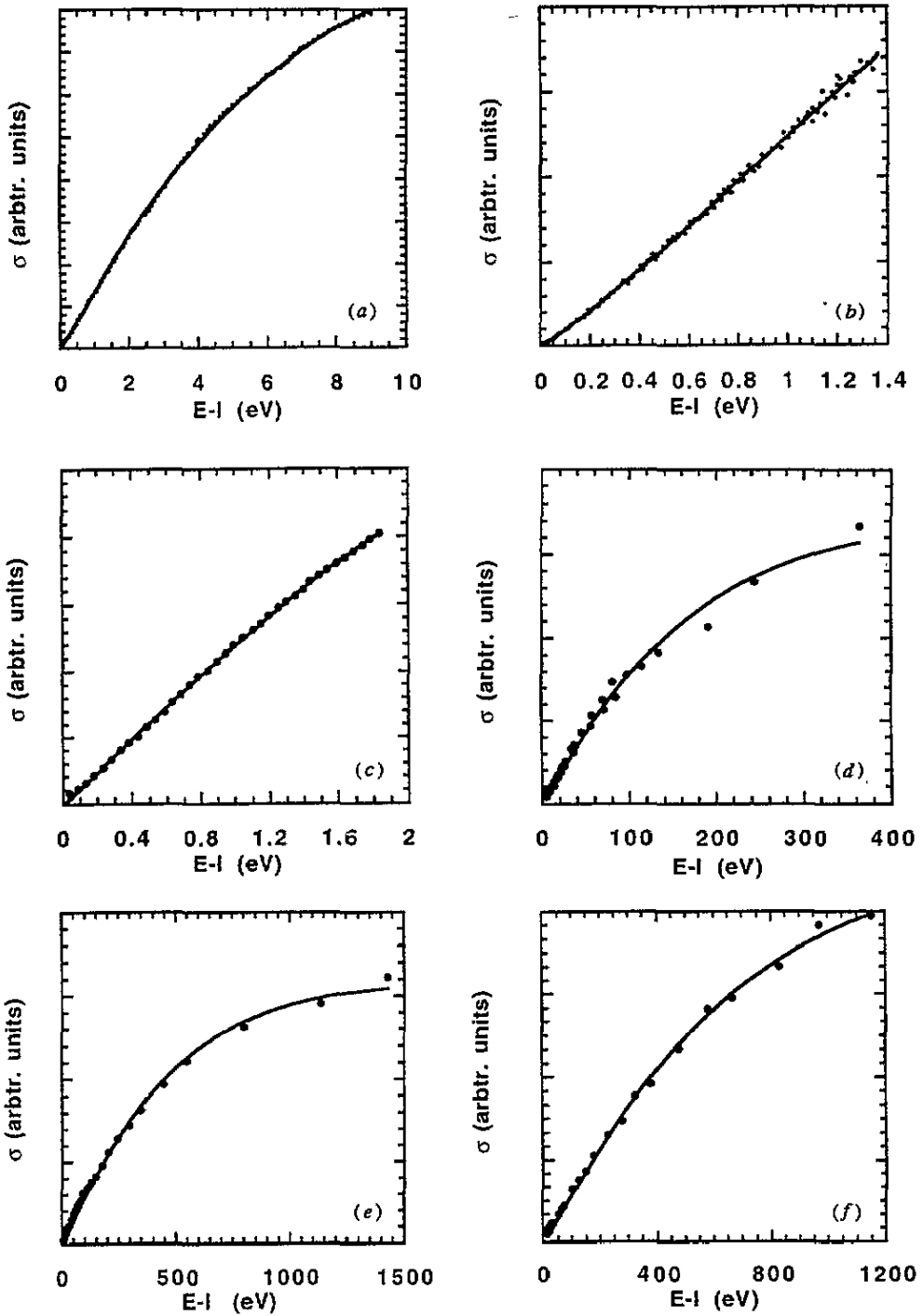


**Figure 11.** Total ionization cross sections in arbitrary units. The full curve is the hydrogen cross section with adapted scaling parameters according to (28). The ionization cross sections (a)–(c) are for the valence shell electrons (a) H(1s) (McGowan and Clarke 1968), (b) He(1s) (Cvejanović and Read 1974) and (c) Na(3s) (Kelley *et al* 1983). In (d)–(f) inner-shell ionization is shown for (d) Ne(1s) (Kamm *et al* 1994), (e) Ar(1s) and (f) Xe(2p) (both Hippler *et al* 1983).

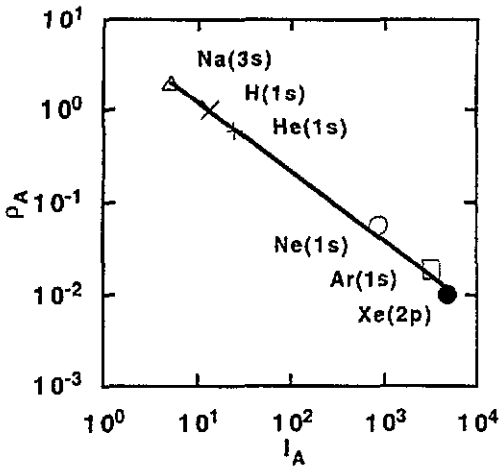


Figure 12. The energy scaling parameter  $\rho$  plotted versus the ionization potential  $I$  for the cross sections from figure 11. The slope of the line in the log-log plot is  $-\frac{3}{4}$ .

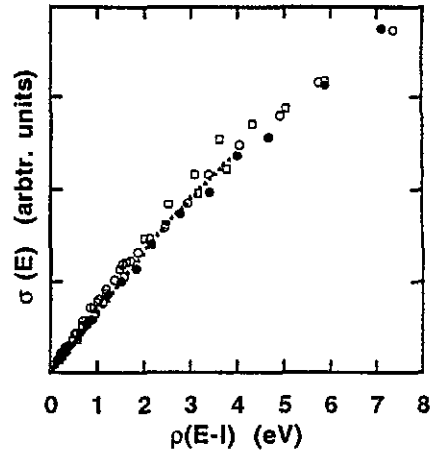


Figure 13. All experimental cross sections from figure 12 scaled according to  $\rho(I)$  from (29) to the energy scale of hydrogen, (x) H(1s), ( $\Delta$ ) Na(3s), ( $\circ$ ) Ne(1s), ( $\square$ ) Ar(1s), and ( $\bullet$ ) Xe(2p).

$\rho_A = \rho(I_A)$  is linear with a slope of of  $-\frac{3}{4}$  (figure 12) so that we may approximate

$$\rho(I) = \left( \frac{13.6\text{eV}}{I} \right)^{3/4}. \quad (29)$$

Together with (28) only the absolute scale of the individual cross sections  $\sigma_A$  remains undetermined. However, as already mentioned above, the absolute cross section is not measured in most threshold experiments. To demonstrate the validity of (29) we show in figure 13 all experimental cross sections from figure 11, scaled to the hydrogenic cross section according to (29).

### 6.3. Comment on the threshold behaviour of inner-shell ionization

The present results indicate that the cross section for any threshold ionization behaves like the hydrogenic cross section characterized with the Wannier exponent  $\alpha$ . Particularly for inner-shell ionization this deserves some explanation. The electron pair leaving the atom from an inner-shell region must penetrate the entire atomic electron cloud (Klar 1981). Slow electrons might be passed by the Auger electron following the decay of the inner-shell hole. Subsequently, the slow ionized electron will see a core whose charge has increased by one and it is conceivable that a significant fraction of the slow electrons will not escape but fall back into the nucleus. These hindered ionization events should change the ionization characteristics compared to a structureless target. Why do such processes not alter the energy dependence of the cross section? The energy sharing function (7) provides an explanation. This function is relatively smooth (from threshold to 8 eV excess energy in hydrogen the maximum difference between the probability for an electron with energy  $\epsilon \approx 0$  and  $\epsilon \approx E/2$  is not more than 8% (compare with figure 5(c) of Rost (1994)). In a crude approximation we could assume that the energy sharing is constant. In this case, the eventually missing tail of slow electrons in the energy sharing distribution of the ionization yield of inner-shell electrons will mainly affect the absolute value of the signal (which is represented by  $\beta_A$  in (28)) but not the functional energy dependence of the total ionization cross section.

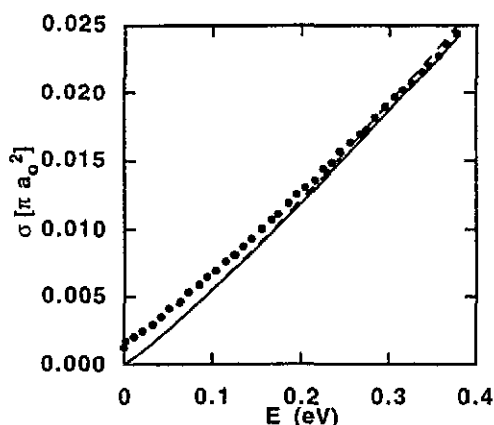


Figure 14. Detail of figure 10 for the threshold region  $0 \leq E \leq 0.4$  eV.

#### 6.4. The determination of the power law in experimental cross sections

One goal in the analysis of experimental threshold cross sections has always been to confirm or contradict the Wannier law  $E^{1.127}$  of the total cross section. In many experimental situations the threshold itself is a problematic region due to finite energy resolution and do to the uncertainty in the position of the threshold. In this situation the power law has been applied to some finite energy region above threshold. This is the main reason for the discrepancies which have been reported for the threshold exponent  $\alpha$  from different experiments. To determine the threshold exponent correctly it is crucial (i) to have reliable data very close to  $E = 0$  and this implies, in turn, that (ii) it is necessary to know precisely where  $E = 0$  is in the experiment and (iii) that the theoretical curve must be convoluted with the experimental energy resolution. In practice, this is impossible and the dilemma can only be avoided if the shape of the cross section is known for a wider energy range than just at threshold. A magnification of figure 10 for the threshold region in figure 14 highlights, in particular, point (iii). The discrepancy between theory and experiment can be attributed to the energy resolution of 0.1eV in the experiment by McGowan and Clarke (1968).

Here we have assumed that we know the (universal) shape of the ionization cross section from the calculation for hydrogen. With this ansatz we could indirectly show that, in fact, all types of threshold cross sections are consistent with the Wannier power law  $\sigma \propto E^{1.127}$ .

## 7. Summary and outlook

This paper documents the first attempts to formulate and apply semiclassical  $S$ -matrix theory to fragmentation under long-range (Coulomb) potentials. We find the results encouraging and hope that they will provide motivation for further studies.

With only a single classical trajectory contributing to a differential cross section, it has been possible to justify an extremely simple version of the semiclassical  $S$ -matrix approach for scattering near the fragmentation threshold. Thereby, the semiclassical  $S$ -matrix has provided a link between Wannier's and others' classical phase space theories and standard quantum mechanical scattering theory.

Besides more applied work of calculating differential cross sections following electron, ion or photon impact, future studies could elaborate on the fundamental question concerning the relation between a quantum mechanical and a semiclassical description. For this

issue scattering below threshold is of particular interest exhibiting such complex classical phenomena as chaotic scattering with fractal structures (Rost and Wintgen 1994). Overall, the results from this work provoke the question: to what extent is electron-atom scattering, not only close to threshold, a (semi)classical process?

### Acknowledgments

I would like to thank J Berakdar, J S Briggs, H Klar, W Mehlhorn and the late D Wintgen for many helpful discussions. The work has been supported by the DFG through SFB 276 at the university of Freiburg.

### Appendix A. Proof of the classical properties of a Coulomb system from section 2.2

Here we briefly sketch the proof of the properties (i)–(iii) which do not appear to be well known. However, specialized to the two-electron atom they can be found explicitly (i) and implicitly (ii,iii) in Wannier's paper from 1953.

(i) To prove that the hyperradius  $\mathcal{R}(t)$  has a single minimum as a function of time we consider the classical Hamiltonian of  $3N - 3$  degrees of freedom (relative motion of  $N$  particles) with a homogeneous potential of degree  $n$  in hyperspherical coordinates

$$H \equiv E = \frac{\mathcal{P}^2}{2} + \frac{\Lambda^2(\Omega)}{2\mathcal{R}^2} + C(\Omega)\mathcal{R}^n \quad (\text{A1})$$

where  $\Lambda^2$  is the squared grand angular momentum operator that acts on the  $N - 1$  hyperangles  $\Omega$ . The angles may be defined in various ways, see for instance Louck (1960). With Hamilton's equations we can write

$$\frac{d\mathcal{P}}{dt} \equiv \frac{d^2\mathcal{R}}{dt^2} = -\frac{\partial H}{\partial \mathcal{R}} = \frac{\Lambda^2(\Omega)}{\mathcal{R}^3} - nC(\Omega)\mathcal{R}^{n-1}. \quad (\text{A2})$$

Using equation (A1) and the fact that  $\mathcal{P} = d\mathcal{R}/dt = 0$  at an extremum we can reformulate (A2) as

$$\left. \frac{d^2\mathcal{R}}{dt^2} \right|_{\dot{\mathcal{R}}=0} = \left(1 + \frac{n}{2}\right) \frac{\Lambda^2(\Omega)}{\mathcal{R}^3} - \frac{nE}{\mathcal{R}}. \quad (\text{A3})$$

One sees from (A3) that for  $n = 0, -1, -2$  the second derivative of  $\mathcal{R}(t)$  at the extremum (if it exists) is positive provided that  $E > 0$ . In these cases each trajectory has a single minimum in the hyperradius (because *all* extrema would be minima according to (A3) and  $\mathcal{R}(t)$  is differentiable). The solution corresponds to the dipole potential ( $n = -2$ ), the Coulomb potential ( $n = -1$ ) and the trivial case of free motion ( $n = 0$ ). Additional solutions occur for  $E < 0$ . Mathematically a single minimum in  $\mathcal{R}(t)$  may exist if  $n > 0$ . Physically it is simply the 'centre' of attraction of the multidimensional but attractive and homogeneous potential. From the structure of the proof it is clear that the result holds for arbitrary masses of the  $N$  particles.

(ii) In the scaled Hamiltonian (4) the scaled grand angular momentum operator  $\tilde{\Lambda}$  has an implicit dependence upon the total scaled angular momentum  $\tilde{L}$  but not on the energy  $E$ ,  $\tilde{\Lambda}(\Omega) = \tilde{\Lambda}(\Omega, \tilde{L})$ . From equation (3) we know that  $\tilde{L} = E^{1/2}L$ . Hence, for any finite  $L$ , we have  $\lim_{E \rightarrow 0} \tilde{\Lambda}(\Omega, \tilde{L}) = \tilde{\Lambda}(\Omega, 0)$  which is independent of the total angular momentum  $L$  and coincides with  $L = \tilde{L} = 0$ . Therefore all partial waves  $L$  in (A1) are described by the  $L = 0$  partial wave for  $E \rightarrow 0$ .

(iii) This property follows from the equations of motion for  $p_\theta$  with the appropriate initial conditions  $\theta(t_0) = 180^\circ$  and  $p_\theta(t_0) = 0$ . However, it holds only for three particles,  $N = 3$ .

## Appendix B. Proof of the identical action for a direct and an exchange orbit

We start from the initial state consisting of a bound (Kepler) orbit denoted by  $\alpha'$  and a free projectile with momentum  $p'_1$ . We want to prove that the action for an orbit that goes from this initial state to a final continuum state with momenta  $p_1, p_2$  is the same as for an orbit which starts with the same initial state but ends at a final state with *exchanged* electrons,  $p_2, p_1$ . The action differential  $d\Phi = r_1 dp_1 + r_2 dp_2$  itself is symmetric under electron exchange. We have to prove that

$$\int_{p'_1, p'_2}^{p_1, p_2} d\Phi = \int_{p'_1, p'_2}^{p_2, p_1} d\Phi \quad (\text{B1})$$

where  $p'_2$  denotes the initial momentum on the Kepler ellipse. Interchanging the indices  $1 \leftrightarrow 2$  on the right-hand side of (B1) reveals that (B1) is valid if  $p'_1 = p'_2$ . Since  $p'_1$  is fixed by the projectile energy we must be able to choose the initial momentum on the Kepler ellipse  $p'_2 = p'_1$ . This choice is indeed always possible for two reasons. Firstly, in principle all momenta  $p'_2 \in ]-\infty, \infty[$  are available along a Kepler ellipse. Secondly, the discussion of the initial conditions in section 3.3 has revealed that we are free to choose the starting point on the Kepler ellipse. Hence, the condition  $p'_1 = p'_2$  can always be fulfilled and the action of the direct and the exchanged path are indeed identical.

## References

- Abrines R and Percival I 1966 *Proc. R. Soc.* **88** 861  
 Baranger H U, Jalabert R A and Stone A D 1993 *CHAOS* **3** 665  
 Berakdar J and Briggs J S 1994 *Phys. Rev. Lett.* **72** 3799  
 Blümel R and Reinhardt W P 1991 *Directions in Chaos* ed B L Hao, D H Feng and J M Yuan (Singapore: World Scientific)  
 Boesten L G J, Banks D and Heideman H G M 1976 *J. Phys. B: At. Mol. Phys.* **9** L97  
 Boesten L G J, Heideman H G M, Bensen T F M and Banks D 1976 *J. Phys. B: At. Mol. Phys.* **9** L1  
 Brauner M, Briggs J S and Klar H 1989 *J. Phys. B: At. Mol. Opt. Phys.* **22** 2265  
 Bray I and Stelbovics A T 1993 *Phys. Rev. Lett.* **70** 746  
 Brink D M 1982 *Semiclassical Methods for Nucleus-Nucleus Scattering* (Cambridge: Cambridge University Press)  
 Burke P G and Berrington K A (eds) 1993 *Atomic and Molecular Processes: an R-matrix Approach* (Bristol: Institute of Physics Publishing)  
 Crothers D S 1986 *J. Phys. B: At. Mol. Phys.* **19** 463  
 Cvejanović S and Read F H 1974 *J. Phys. B: At. Mol. Phys.* **7** 1841  
 Dimitrijević S and Grujić P 1983 *J. Phys. B: At. Mol. Phys.* **16** 297  
 Du M L and Delos J B 1987 *Phys. Rev. Lett.* **58** 1731  
 Eckhardt B 1991 unpublished  
 Ezra G S, Richter K, Tanner G and Wintgen D 1991 *J. Phys. B: At. Mol. Opt. Phys.* **24** L413  
 Feagin J M 1984 *J. Phys. B: At. Mol. Phys.* **17** 2433  
 Ford K W and Wheeler J A 1959 *Ann. Phys., NY* **7** 259  
 Gailitis M 1986 *J. Phys. B: At. Mol. Phys.* **19** L697  
 Gaspard P and Rice S A 1993 *Phys. Rev. A* **48** 54  
 Goldstein H 1980 *Classical Mechanics* (London: Addison-Wesley)  
 Grujić P 1986 *Commun. At. Mol. Phys.* **18** 47  
 Gu Y and Yuan J M 1993 *Phys. Rev. A* **47** R2442  
 Gutzwiller M C 1990 *Chaos in Classical and Quantum Mechanics* (New York: Springer)  
 Handke G, Draeger M, Ilhwa W and Friedrich H 1993 *Phys. Rev. A* **48** 3699

- Hasegawa H, Robnik M and Wunner G 1989 *Prog. Theor. Phys. Suppl.* **98** 198
- Hippler R, Klar H, Saeed K, McGregor I, Duncan A J, and Kleinpoppen H 1983 *J. Phys. B: At. Mol. Phys.* **16** L617
- Jung Ch 1986 *J. Phys. A: Math. Gen.* **19** 1345
- Kamm M, Weber W, and Mehlhorn W 1994 *J. Phys. B: At. Mol. Opt. Phys.* **27** 2585
- Kazansky A K and Ostrovsky V N 1993 *Phys. Rev. A* **48** R871
- 1994 *J. Phys. B: At. Mol. Opt. Phys.* **27** 5197
- Kelley M H, Rogers W T, Celotta R J, and Mielczarek S R 1983 *Phys. Rev. Lett.* **51** 2191
- Kim J H and Ezra G S 1991 *Quantum Chaos Proc. Adriatico Research Conf. (Trieste)* ed H A Cerdeira, R Ramaswamy, M C Gutzwiller and G Casati (Singapore: World Scientific)
- Klar H 1981 *J. Phys. B: At. Mol. Phys.* **14** 3255
- 1981b *J. Phys. B: At. Mol. Phys.* **14** 4165
- Klar H and Fehr M 1992 *Z. Phys. D* **23** 295
- Louck J D 1960 *J. Mol. Spectrosc.* **4** 298
- Lubell M S 1994 *Z. Phys. D* **30** 79
- Manning R S and Ezra G S 1994 *Phys. Rev. A* **50** 954
- Main J, Wiebusch G, Holle A and Welge K H 1986 *Phys. Rev. Lett.* **57** 2789
- Maslov V P and Fedoriuk M V 1981 *Semi-Classical Approximations in Quantum Mechanics* (Boston: Reidel)
- Maulbetsch F and Briggs J S 1992 *Phys. Rev. Lett.* **68** 2004
- Miller W H 1970 *J. Chem. Phys.* **53** 1949
- 1970b *J. Chem. Phys.* **53** 3578
- 1970c *Chem. Phys. Lett.* **7** 431
- W H 1974 *Adv. Chem. Phys.* **25** 69
- 1975 *Adv. Chem. Phys.* **30** 77
- McGowan J W and Clarke E M 1968 *Phys. Rev.* **167** 43
- Müller J, Burgdörfer J and Noid D 1992 *Phys. Rev. A* **45** 1471
- Peterkop R K 1971 *J. Phys. B: At. Mol. Phys.* **4** 513
- Proulx D and Shakeshaft R 1993 *Phys. Rev. A* **48** R875
- Rankin C C and Müller W H 1971 *J. Chem. Phys.* **55** 3150
- Rau A R P 1971 *Phys. Rev. A* **4** 207
- 1984 *Phys. Rep.* **110** 369
- Read F H 1984 *J. Phys. B: At. Mol. Phys.* **17** 3965
- 1984a *Electron Impact Ionization* ed T D Märk and G H Dunn (New York: Springer) p 42
- Rosenberg L 1973 *Phys. Rev. D* **8** 1833
- Rost J M 1994 *Phys. Rev. Lett.* **72** 1998
- 1994b *Int. Conf. on Few-Body Systems XIV (AIP Conf. Proc.)* at press
- 1994c *J. Phys. B: At. Mol. Opt. Phys.* **27** 5923
- 1994d unpublished.
- Rost J M and Heller E J 1994 *Phys. Rev. A* **49** R4289
- Rost J M and Wintgen D 1994 submitted
- Sepulveda M A and Heller E J 1994 *J. Chem. Phys.* **101** 8004
- Taylor J R 1972 *Scattering Theory* (New York: Wiley)
- Temkin A 1982 *Phys. Rev. Lett.* **49** 365
- Tomsovic S and Heller E J 1993 *Phys. Today* **July** 38 and references therein
- van Vleck 1928 *J. M. Proc. Acad. Natl. Sci., USA* **14** 178
- Wannier G H 1953 *Phys. Rev.* **90** 817
- Weber and Raith 1994 Private communication
- Wetmore A E and Olson R E 1986 *Phys. Rev. A* **34** 2822
- Wigner E P 1948 *Phys. Rev.* **73** 1002
- Wintgen D 1987 *Phys. Rev. Lett.* **58** 1589
- 1988 *Phys. Rev. Lett.* **61** 1803
- Wintgen D, Richter K and Tanner G 1992 *CHAOS* **2** 19
- Wintgen D and Friedrich H 1989 *Phys. Rep.* **183** 37